NeuroImage: Clinical 19 (2018) 690–702

Contents lists available at ScienceDirect

NeuroImage: Clinical

journal homepage: www.elsevier.com/locate/ynicl

Trait related sensorimotor deficits in people who stutter: An EEG investigation of μ rhythm dynamics during spontaneous fluency

David Jenson*, Kevin J. Reilly, Ashley W. Harkrider, David Thornton, Tim Saltuklaroglu

University of Tennessee Health Science Center, Dept. of Audiology and Speech Pathology, United States

ABSTRACT

Stuttering is associated with compromised sensorimotor control (i.e., internal modeling) across the dorsal stream and oscillations of EEG mu (μ) rhythms have been proposed as reliable indices of anterior dorsal stream processing. The purpose of this study was to compare μ rhythm oscillatory activity between (PWS) and matched typically fluent speakers (TFS) during spontaneously fluent overt and covert speech production tasks. Independent component analysis identified bilateral μ components from 24/27 PWS and matched TFS that localized over premotor cortex. Time-frequency analysis of the left hemisphere μ clusters demonstrated significantly reduced μ-α and μ-β ERD ($p_{CLUSTER} < 0.05$) in PWS across the time course of overt and covert speech production, while no group differences were found in the right hemisphere in any condition. Results were interpreted through the framework of State Feedback Control. They suggest that weak forward modeling and evaluation of sensory feedback across the time course of speech production characterizes the trait related sensorimotor impairment in PWS. This weakness is proposed to represent an underlying sensorimotor instability that may predispose the speech of PWS to breakdown.

1. Introduction

Over the last century, the etiology of developmental stuttering has been explained through various psychological and organic paradigms. While genetic sources continue to be investigated (Suresh et al., 2006; Drayna and Kang, 2011; Yairi and Ambrose, 2013), manifestations of core stuttering behaviors (i.e., silent blocks, repetitions, and prolongations of speech sounds) are currently attributed to compromised sensorimotor control (Max et al., 2004a, 2004b; Civier et al., 2010; Civier et al., 2013; Daliri et al., 2014) and related timing (Alm, 2004; Etchell et al., 2014; Falk et al., 2015; Etchell et al., 2016) mechanisms. Sensorimotor control, enabling speech initiation, error correction, and fluent coarticulation, is subserved by a left hemisphere dominant dorsal stream network (Hickok and Poeppel, 2004, 2007) and is reliant on internal models. Forward (i.e., motor to sensory) internal models, containing sensory predictions of the motor plan (Von Holst, 1954; Wolpert and Flanagan, 2001; Crapse and Sommer, 2008), are encoded in projections from anterior motor regions to posterior sensory regions. Forward models are evaluated in posterior sensory regions through parallel internal and external loops, which compare predicted sensory feedback to the sensory target [internal] and available reafference [external] respectively (Hickok et al., 2011; Houde and Nagarajan, 2011). Sensory error signals arising from these comparisons are mapped onto corrective motor commands via sensory to motor projections (i.e., inverse models) and returned to PMC for integration into ongoing motor planning. Sensorimotor control is thought to be disrupted in people who stutter (PWS), possibly because of weak or unstable forward models (Max et al., 2004a, 2004b; Brown et al., 2005), a noisy comparison between the prediction and target (Max et al., 2004a; Hickok et al., 2011), or abnormal reliance on sensory reafference during speech (Max et al., 2004a; Namasivayam et al., 2009). While it is thought that stuttering behaviors arise from this compromised internal modeling mechanism, it remains unclear how these deficits can be observed in fluent speech.

Imaging data generally support notions of an underlying internal modeling deficit in stuttering. Neuroanatomical differences between PWS and typically fluent speakers (TFS) include reduced left hemisphere gray matter volume in anterior motor (Beal et al., 2007; Chang et al., 2008; Beal et al., 2013) and posterior auditory regions (Foundas et al., 2001), accompanied by reduced white matter density in the fiber tracts linking them (Sommer et al., 2002; Chang and Zhu, 2013; Chang, 2014; Connally et al., 2014; Cieslak et al., 2015). Increased gray matter volume in right hemisphere motor (Beal et al., 2013) and auditory (Beal et al., 2007) homologues coupled with increased white matter density in the fiber tracts connecting them (Beal et al., 2007; Chang et al., 2011; Cai et al., 2014) have been interpreted as evidence of right hemisphere

* Corresponding author.
E-mail address: djenson1@uthsc.edu (D. Jenson).

https://doi.org/10.1016/j.nicl.2018.05.026
Received 13 October 2017; Received in revised form 28 March 2018; Accepted 20 May 2018
Available online 21 May 2018

compensation (Preibisch et al., 2003; Neumann et al., 2005). Several findings, however, suggest that the internal modeling deficit in PWS deserves further investigation. First, functional studies have reported both hyperactivation (Ingham et al., 2000; Brown et al., 2005; Loucks et al., 2011; Ingham et al., 2012) and hypoactivation (Watkins et al., 2008; Chang et al., 2009; Kell et al., 2009; Loucks et al., 2011; Toyomura et al., 2011) in left anterior dorsal regions. Second, while weak forward modeling in PWS is supported by reports of reduced speech induced auditory suppression (Numminen et al., 1999; Curio et al., 2000) of the N100 response (Daliri and Max, 2015a, 2015b, 2016), other studies have failed to show this (Beal et al., 2010; Beal et al., 2011). Thus, further investigation is needed to clarify the mechanism by which the aberrant neurophysiology in PWS gives rise to the deviant speech patterns characteristic of the disorder.

Complicating interpretation of equivocal findings in PWS is the difficulty in separating state- (differences between the fluent and disfluent speech of PWS) and trait- (differences between PWS and fluent controls when stuttering is eliminated) based effects of stuttering (Belyk et al., 2015). Identification of trait-based differences requires the comparison of fluent speech from PWS and TFS to eliminate the potentially contaminating effects of stuttered speech on neural activity. The intermittent and unpredictable nature of stuttering is therefore problematic for PET and fMRI, as they lack the temporal resolution to delineate neural activity pertaining to fluent and stuttered portions of the same utterance (Ingham et al., 2012). Additionally, several fMRI studies which purported to use spontaneously fluent speech have acknowledged the potentially fluency enhancing effect of scanner noise (Neumann et al., 2003; Preibisch et al., 2003; Giraud et al., 2008; Howell et al., 2012). Consequently, some trait-based studies have induced fluency in PWS through delayed auditory feedback (Sakai et al., 2009), choral speech (Fox et al., 2000; Watkins, 2011), or by altering normal speech patterns (Braun et al., 1997; Kell et al., 2009). Investigation of trait-based effects using induced fluency is questionable, as it is unclear whether the neurophysiology supporting induced fluency accurately represents normal function of the speech network in PWS. The analysis of neural data from spontaneously fluent speech represents a unique opportunity for probing trait-based, neurophysiologic differences in stuttering that are free from the potentially contaminating effect of overt stuttering, but still reflect the normative state of sensorimotor processing in PWS. Thus, in order to better test the hypothesis that deficient forward modeling and processing of sensory feedback constitute trait-related aspects of stuttering, there is a need for temporally precise neural data recorded during spontaneously fluent speech in quiet backgrounds.

The electroencephalographic (EEG) mu (μ) rhythm is a prime avenue for interrogating internal modeling for speech production. It is commonly recorded over anterior dorsal stream regions (Tamura et al., 2012; Jenson et al., 2014), including the premotor cortex, which serves as a computational hub for processing sensorimotor information (Hickok et al., 2011; Tourville and Guenther, 2011; Guenther and Vladusich, 2012). The μ rhythm is characterized by spectral peaks in alpha (α; ~10 Hz) and beta (β; ~20 Hz) frequency bands. Suppression (event related desynchronization; ERD) of activity in the β band is a ubiquitous finding during motor tasks (Alegre et al., 2006; Erbil and Ungan, 2007; Brinkman et al., 2014; Heinrichs-Graham et al., 2014; Cuellar et al., 2016), and has been linked to motor execution (Seeber et al., 2014). However, sensorimotor β (μ-β) power also has been found to be modulated prior to (Gehrig et al., 2012) and following (Tan et al., 2014; Tan et al., 2016) movement, and is independent of muscle force (Stancak et al., 1997; Pistohl et al., 2012; Kilavik et al., 2013). These findings and the fact that μ-β can also suppress in action perception (Babiloni et al., 2002; Muthukumaraswamy and Johnson, 2004; Hari, 2006) and imagination (Brinkman et al., 2014; Yi et al., 2016; Di Nota et al., 2017), has provided strong support for μ-β activity encoding motor to sensory (i.e., forward) models (Moisello et al., 2015; Mersov et al., 2016). Similar to μ-β, μ-α also suppresses in response to movement (Dziewas et al., 2003; Rektor et al., 2006; Nakayashiki et al., 2014; Seeber et al., 2014; Cuellar et al., 2016; Duann and Chiou, 2016; Wagner et al., 2016), and has been considered a primary somatosensory response (Jones et al., 2009). However, μ-α power also has been found to be sensitive to changes in visual (Oberman et al., 2005; Sabate et al., 2012), somatosensory (Hari, 2006; Quandt et al., 2013), and auditory (Tamura et al., 2012; Pineda et al., 2013; Jenson et al., 2014; Jenson et al., 2015) feedback and has been considered an index of mirror neuron activity (Arnstein et al., 2011; Braadbaart et al., 2013), providing strong evidence that μ-α is sensitive to sensory to motor feedback changes.

A number of recent studies have used independent component analysis (ICA; Stone, 2004; Onton et al., 2006) to identify μ rhythms with characteristic α and β peaks in speech perception and production tasks (Bowers et al., 2013; Jenson et al., 2014; Jenson et al., 2015; Saltuklaroglu et al., 2017; Thornton et al., 2017). Time-frequency analyses provided measures of event-related synchronization and desynchronization (ERS and ERD) of μ-α and μ-β over the time course of speech events. Changes in oscillatory power over time were interpreted as contributions from forward modeling (μ-β) and sensory feedback (μ-α). In speech production tasks, ICA is an effective means of separating electromyographic (EMG) artifact from neural activity. Jenson et al. (2014, 2015) identified the sensorimotor μ and a separate perilabial (EMG) component, such that time-frequency dynamics of μ components could be temporally referenced to muscle movements. μ-α and μ-β ERD emerged during speech preparation and were observed most robustly in the left hemisphere with the onset of EMG activity and persisting throughout the utterance. The left hemispheric dominance of activity in these findings further supports their application to measuring sensorimotor control in speech. These data can be interpreted through State Feedback Control (SFC; Houde and Nagarajan, 2011) theory which proposes that forward models are generated in premotor regions and evaluated in posterior sensory regions across the time course of speech production, with sensory feedback being returned to premotor regions even in the absence of an overt error (Niziolek et al., 2013). Based on these findings and interpretations, a logical next step for understanding trait-related sensorimotor differences associated with stuttering is the comparison of μ rhythm activity between stuttering and non-stuttering individuals when producing spontaneously fluent speech.

Because μ rhythms can capture both primary motor and somatosensory as well sensorimotor responses in movement tasks, one way to isolate sensorimotor responses in speech may be to remove movement and use covert production tasks. Though covert speech does not require movement or generate reafferent feedback, forward models of the speech target and expected sensory feedback are incurred via a purely internal loop (Tian and Poeppel, 2010; Houde and Nagarajan, 2011; Tian and Poeppel, 2012). In support of this, Jenson et al. (2014) found that μ rhythm responses to covert speech showed similar, albeit weaker ERD responses to those of overt speech. Thus, covert production tasks enable the interrogation of internal sensorimotor loop dynamics without the influences of obligatory motor and somatosensory responses or reafferent feedback. If, as has been proposed, forward modeling deficits in PWS lead to an overreliance on sensory feedback (Max et al., 2004a, 2004b), then time-frequency decomposition of μ rhythm activity associated with both covert and overt speech tasks is likely to provide a more robust understanding of stuttering-related sensorimotor deficits.

Previous investigation of the μ rhythm in PWS has demonstrated its capacity for revealing sensorimotor differences underlying the disorder. Saltuklaroglu et al. (2017) identified differential activity in PWS across both μ-α and μ-β bands during accurate speech and tone discrimination in noise, interpreting them as evidence of a sensorimotor inflexibility rooted in a reduced capacity for forward modeling. The presence of reduced spectral power in the μ-β band across conditions was interpreted to suggest a general, rather than speech-specific, sensorimotor deficit. This is consistent with the findings of Joos et al. (2014), who

reported reduced μ-β spectral power during resting state, raising the possibility that spectral differences may constitute a neural biomarker for stuttering. However, it should be noted that μ-β power was not correlated with stuttering severity in either study. Consequently, the relationship between μ-β rhythms and the manifestation of stuttering events remains unclear.

The goals of the current study are first to identify and temporally decompose μ rhythm and EMG components from EEG recordings made during overt and covert speech in PWS and matched TFS cohorts. Following identification, the second goal is to temporally decompose μ component activity such that μ rhythm fluctuations are mapped to the onset of lip movement. Between-group comparisons will examine the extent to which spontaneously fluent overt and covert speech of PWS is marked by weak forward modeling and overreliance on sensory feedback with time-frequency analyses of μ-β and μ-α serving as indices of forward modeling and sensory feedback processing, respectively. It is first hypothesized that, if the fluent speech of PWS is characterized by weak forward modeling (Max et al., 2004a, 2004b; Hickok et al., 2011), group differences will be found in the μ-β band activity during overt speech production. Second, it is hypothesized that, if the sensorimotor impairment relates to the prediction and evaluation of sensory feedback supported by the internal loop, then both μ-α and μ-β band differences will be present during covert speech tasks when no reafference is available to update the forward model and sensory guidance is based exclusively on motor to sensory forward model predictions. Support for these hypotheses will more clearly describe the underlying neural impairment in PWS free from the state-based effects of disfluency. The findings are expected to facilitate development of novel therapeutic interventions.

2. Methods

2.1. Participants

Thirty-one adult native English speakers (26 right handed) with developmental stuttering were recruited from the University of Tennessee and the surrounding Knoxville area. PWS (22 male, 9 female) had a mean age of 26.1 (range 17–53), and no history of cognitive, communicative, or attentional disorders apart from persistent developmental stuttering. Four PWS were excluded from the analysis as they were not able to complete the experimental tasks (discussed below), while a further three did not yield usable left or right μ components. Thus, data from only 24 of the original 31 PWS was included in the between group analysis.

Age (within 3 years) and gender matched control subjects (23 right handed) were recruited for all 24 PWS who produced μ components. Matched control subjects had a mean age of 26.2 (range 18–44) and reported no history of cognitive, communicative, or attentional disorders. Handedness dominance was assessed with the Edinburgh Handedness Inventory (Oldfield, 1971). This study was approved by the Institutional Review Board for the University of Tennessee, and all subjects provided informed consent prior to participation in the study.

2.2. Stimuli

Visual stimuli for all conditions were presented in the center of the subjects' visual field on Microsoft PowerPoint slides. Stimuli were presented in white text on a black background, subtending a visual angle of 1.14°. Disappearance of the visual stimuli following a two second visual presentation served as the cue to initiate production. The timeline for the production conditions can be seen in Fig. 1.

2.3. Design

The experiment consisted of a 2 × 3 mixed design. The three conditions were:

1. Covert production of syllable pairs (SylC)
2. Overt production of syllable pairs (SylP)
3. Overt production of tri-syllable nouns (WordP)

Conditions 1 and 2 (SylC and SylP) required covert and overt production of syllable pairs consisting of /ba/ and /da/, respectively. In order to maximize fluent productions, syllable pairs were chosen as they are less likely to be stuttered due to their short duration (Brown, 1945). Condition 3 (WordP) required overt production of tri-syllable nouns initiated by either /b/ or /d/ and followed by a vowel. Stimuli for the WordP condition were selected from Blockcolsky et al. (2008). Tri-syllable nouns were included in order to increase the complexity and ecological validity of the speech tasks. Both sets of stimuli have been shown previously to lead to salient markers of speech onset and offset (Jenson et al., 2014; Jenson et al., 2015), enabling interpretation of neural activity across the time course of speech events.

2.4. Procedure

Prior to conducting the experiment, all PWS completed the Stuttering Severity Instrument–4th edition (SSI-4) (Riley, 2009). SSI administration took place prior to experimental participation to mitigate against potential carry-over fluency (Saltuklaroglu and Kalinowski, 2011) due to the design of the experiment. Speech samples for the SSI were analyzed by two graduate students under the supervision of a clinically–certified Speech-Language Pathologist.

The experiment was conducted in an electrically and magnetically shielded, double-walled soundproof booth fit with a faraday cage. Subjects were seated in a reclining chair with their head and neck well supported. Stimulus presentation for all conditions was accomplished via Compumedics NeuroScan Stim 2 version 4.3.3, running on a PC computer.

In all production conditions, subjects were instructed to initiate their productions following the disappearance of the visual stimuli. In the covert production condition (SylC), subjects were instructed to refrain from making any silent articulatory gestures during their covert productions. For the overt production conditions (SylP, WordP), verbal responses from PWS were recorded on a digital voice recorder (RCA model VR5340-A) to enable offline analysis of speech fluency. All subjects were instructed to produce the speech targets in their normal speaking voice, with PWS further instructed not to employ any fluency enhancing techniques. Any trials in which the production was not completed within the 2000 ms window between response cue and the end of the trial epoch were discarded. Each of the three conditions was presented in 2 blocks of 40 trials each, yielding a total of 6 blocks (3 conditions × 2 blocks). Block presentation order was randomized across subjects.

2.5. Data acquisition

Whole head EEG data were recorded from a 68 channel NeuroScan Quikcap based on the 10–10 extension (Chatrian et al., 1988) of the international standard system (Jasper, 1958). Neural channels were accompanied by two electrocardiogram (EKG) and two electromyography (EMG) channels. Recording channels were re-referenced to the linked mastoid channels (M1, M2) for common mode noise reduction. The electro-oculogram was captured by two pairs of recording electrodes placed above and below the left eye (VEOU, VEOL) as well as on the medial and lateral canthi of the left eye (HEOL, HEOR) which recorded vertical and horizontal eye movements, respectively. The two EMG electrodes were placed above and below the lips in order to capture speech related peri-labial muscle activity (Gracco, 1988).

EEG data were acquired using Compumedics NeuroScan 4.3.3 software coupled with the Synamps 2 system. Data were band pass filtered (0.15–100 Hz) prior to digitization by a 24 bit analog to digital converter with a sampling rate of 500 Hz. Data collection was

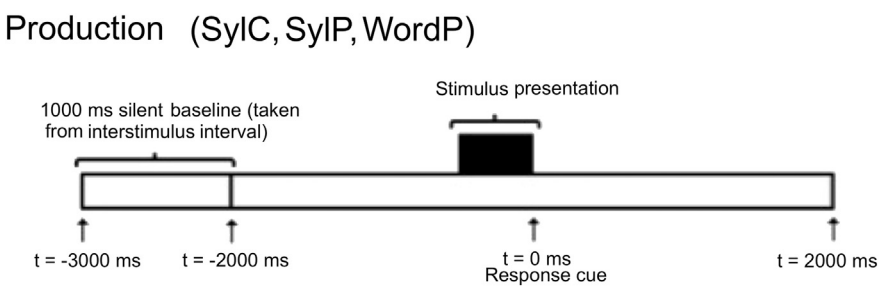

Fig. 1. 5000 ms epoch timelines for single trials in covert (SylC) and overt (SylP, WordP) production conditions.

referenced to the cue to initiate production (i.e., the disappearance of the visual stimulus), thus, time zero represents the initiation cue.

2.6. Preprocessing

All EEG data processing was performed in EEGLAB 13.5.4b (Brunner et al., 2013), an open source MATLAB toolbox. Data for each participant were processed at the individual level, then analyzed at both the individual and group levels. Steps performed at each stage are outlined below:

Individual Processing:

1. Preprocessing of 6 raw files for each subject (2 blocks × 3 conditions).
2. ICA of concatenated data files for each participant.
3. Localization estimation via fitting of equivalent current dipole (ECD) models for all neural and non-neural (i.e., myogenic and movement artifact) components.

Group Analysis

1. Similar components across subjects clustered by Principal Component Analysis (PCA) on the basis of commonalities in spectra, scalp maps, and dipole location.
2. Visual inspection of clusters resulting from PCA to identify left and right μ clusters and validate cluster membership. Neighboring clusters were also examined to identify mis-allocated components.
3. Time-frequency decomposition of left and right μ clusters performed by Event Related Spectral Perturbation (ERSP) analysis.
4. Cluster localization performed by ECD and current source density (CSD) methods.

2.7. Individual analysis

2.7.1. Fluency analysis

Prior to the analysis of neural data, the audio recordings of PWS from the overt production conditions (SylP and WordP) were analyzed and each trial was coded as either fluent or disfluent. Trials were marked as disfluent if they contained syllable repetitions, prolongations, excess tension, or if the response latency indicated that the subject may have had difficulty initiating speech. Trials identified as disfluent were removed at a later stage of the processing pipeline.

2.7.2. Data preprocessing

Both raw data files for each condition (one per block) were appended to create a single file for each condition per subject. The data were then decimated to 256 Hz to reduce the computational demands of further processing steps. All EEG data were referenced to the mastoid channels (M1, M2) for common mode noise reduction. The data were band pass filtered between 3 and 34 Hz in order to reduce gross muscle artifact and to allow clear visualization of the α and β frequency bands. Five-second trial epochs (ranging from −3000 ms to +2000 ms around time zero) were then extracted from the continuous data. The resulting data files for each subject were visually inspected, and all epochs containing gross artifact (> 200 μV) were removed from the data. For PWS, any remaining trial epochs that had been identified as disfluent during the fluency analysis were removed. A minimum of 40 usable trials per condition per participant was required for an effective ICA decomposition.

2.7.3. ICA

Prior to ICA analysis, data files for each subject were concatenated to generate a single set of ICA weights common to all conditions. This enabled the analysis of conditional differences within common spatially fixed components. The data matrix was initially decorrelated by means of an extended Infomax algorithm (Lee et al., 1999). Following decorrelation, ICA training was performed in EEGLAB 13.5.4 via the "extended runica" algorithm with the initial learning weight set to 0.001 and a stopping weight of 10^{-7}. The ICA decomposition yielded 66 ICs for each subject, corresponding to the number of channels submitted to ICA (68 recording channels minus two mastoid reference channels). These components represent the decomposition of the scalp-recorded signal (i.e. neural, EKG, EMG, and electro-oculogram) into temporally independent and spatially fixed components accounting for the original signal. The inverse weight matrix (W^{-1}) was then projected back onto the original spatial channel configuration to generate scalp maps for each component.

Following ICA decomposition, equivalent current dipole (ECD) models for each component were computed by using the BESA (4 shell spherical) head model in the DIPFIT2 toolbox, an open-source MATLAB plugin available at sccn.ucsd.edu/eeglab/dipfit.html (Oostenveld and Oostendorp, 2002). Electrode locations conforming to the 10–10 system (Chatrian et al., 1988) were warped to the head model. Coarse fitting to the BESA head model yielded single ECD models for each of the 3168 components, (66 components × 48 subjects). Localization of cortical activity via ECD models entails back projecting the IC signal to a hypothesized neural source capable of generating the scalp-recorded signal (Delorme et al., 2012). Forward projections of each source signal to the level of the scalp were then compared to the IC scalp maps (Richards, 2004). The residual variance (RV) is the percentage difference between the scalp recorded signal and the forward projection of the ECD model, which can be seen as a measure of the goodness of fit for the ECD models.

2.8. Group analysis – STUDY

The EEGLAB STUDY module was used to perform all group level analyses, as it enables comparison of ICA data across conditions and between groups. ICs were initially preclustered based on similarities in scalp map, spectra, and dipole location. Principal Component Analysis (PCA) was implemented via the K-means statistical toolbox, allocating the ICs to 40 component clusters. These clusters included all neural (e.g., μ) components originating within the skull and non-neural (e.g., peri-labial EMG of interest and other artifactual activity such as eye blinks) components originating outside the skull (Jenson et al., 2014). From the results of PCA, left and right μ clusters were selected for time-frequency analysis.

2.8.1. Mu cluster membership

All components allocated to μ clusters by PCA were evaluated in relation to the inclusion criteria of a characteristic μ spectrum, RV < 20%, and ECD localization across the sensorimotor cortex (BA 1, 2, 3, 4, 6). Components not meeting these inclusion criteria were removed from μ clusters. Additionally, neighboring clusters were visually inspected, with components meeting the inclusion criteria being reallocated to μ clusters (Saltuklaroglu et al., 2017). As 66 recording channels yield the same number of ICs (Makeig et al., 2004), it was possible for participants to contribute multiple components to each cluster. Final allocation of components to μ clusters was verified by a second rater to ensure reliability of cluster membership.

2.8.1.1. Mu cluster source localization. While ECD dipole location (generated via DIPFIT2) was submitted to PCA in the STUDY module, final localization of left and right μ clusters was implemented via standardized low-resolution brain electromagnetic tomography (sLORETA). sLORETA solves the inverse problem by using current source density (CSD) measured from scalp recorded EEG to evaluate source location (Pascual-Marqui, 2002). CSD solutions are based on the Talairach cortical atlas, digitized at the Montreal Neurological Institute (MNI). Electrode locations were cross-registered between realistic cortical anatomy and spherical (BESA) head models (Towle et al., 1993). The cortical volume was divided into 6239 voxels with a spatial resolution of 5 mm. The inverse weight projections of the original EEG signal for each component contributing to left and right μ clusters were exported to sLORETA. Cross spectra were computed and mapped to the Talairach atlas and cross-registered with MNI coordinates corresponding to the MNI152 template (Mazziotta et al., 2001), resulting in CSD source estimates for each component contributing to left and right μ clusters.

To ascertain the statistical significance of differences in CSD estimates across participants, a non-parametric analysis was implemented in the sLORETA software package. The probability distribution of the *t*-statistic expected under the null hypothesis was estimated via randomization (Pascual-Marqui, 2002), correcting for multiple comparisons across all voxels and frequencies (3–34 Hz). Voxels significant at $p < 0.001$ were considered to be active across participants. While cluster localizations are based on CSD source estimates generated with sLORETA, ECD dipole locations are reported both as a reliability measure and to demonstrate the individual variability present in the subject pool.

2.8.2. EMG cluster membership

The peri-labial EMG component for each subject was identified by computing the correlation coefficients between the time-domain signals from the original peri-labial EMG channel and those of all 66 components derived from ICA for each participant. The component demonstrating the highest correlation with the original peri-labial channel was selected as the peri-labial EMG component for each subject. Component selection was then verified by the presence of oscillatory activity in the overt production conditions but not in the covert condition. The residual variance threshold for inclusion to this cluster was raised to 50% as myogenic activity incurs higher levels of localization uncertainty (Gramann et al., 2010). A new cluster was created that included EMG components for each participant such that group averaged time-frequency measures could be computed.

2.8.3. Component measures – ERSP

ERSP analyses were conducted to quantify fluctuations in spectral power (in normalized dB units) across the trial epochs in the frequency bands of interest. Time-frequency transformations were generated with a Morlet wavelet rising linearly from three cycles at 3 Hz to 25.6 cycles at 34 Hz. Spectral perturbations were referenced to a silent 1000 ms baseline taken from the inter-trial interval. A surrogate distribution was constructed from 200 randomly sampled time points within this baseline period, against which individual ERSP changes were generated with a bootstrap resampling method with a threshold of $p < 0.05$ (uncorrected). Data from all experimental conditions from 5 to 30 Hz and between −500 and 1500 ms were included in the ERSP analysis.

Group differences were evaluated with unpaired permutation statistics (2000 permutations) with a significance threshold of $p < 0.05$. Cluster-based corrections for multiple comparisons (Maris and Oostenveld, 2007) were used to control the Type 1 error rate. Statistical analyses consisted of 3 between-groups contrasts (one per condition). To examine a potential relationship between μ time-frequency power and stuttering severity, a Pearson correlation analysis was performed within the PWS group between raw SSI scores and mean spectral power across time-frequency voxels demonstrating significant group differences. Raw SSI scores were used as they are robust measures of severity sensitive to frequency, duration, and behavioral concomitants. Separate correlation analyses were performed for each condition demonstrating group differences. For subjects contributing more than one component to μ clusters, spectral power was averaged across components.

3. Results

3.1. Production accuracy

Two PWS were excluded from the study prior to analysis of neural data due to their inability to produce a minimum of 40 spontaneously fluent utterances in at least one of the overt production conditions. One of the excluded subjects was rated by the SSI as very severe (raw SSI = 44), while the other was rated as mild (raw SSI = 19), though was highly disfluent during study participation. As the analysis software was not amenable to missing data, subjects had to produce usable data in all conditions to be included in the analysis. Inclusion of partial datasets would have skewed statistical results. Two additional PWS were excluded from the study as analysis of their peri-labial EMG activity indicated that they initiated speech production at the onset of the visual prompt as opposed to stimulus offset as instructed. This resulted in neural data from 27/31 PWS being submitted to ICA/ERSP analysis. Table 1 shows the demographic information, severity rating, raw SSI score, and cluster contributions for the PWS included in the ICA/ERSP analysis. Table 2 shows the demographic information and cluster contribution for each of the TFS included in the study.

3.2. Number of usable trials

For the PWS contributing to μ clusters, the average number of usable trials (i.e., fluent and devoid of artifact) per condition were: SylC = 59 (SD = 5.78), SylP = 57.83 (SD = 4.21), and WordP = 57.21 (SD = 4.5). For the TFS contributing to μ clusters, the average number of usable (i.e., devoid of artifact) trials were: SylC = 59.82 (SD = 5.78), SylP = 61.68 (SD = 4.79), and WordP = 62.59 (SD = 6.51). A mixed model repeated measures ANOVA revealed a main effect of group [$F(1,44) = 8.041$; $p = 0.007$], with more usable trials for TFS (mean = 61.3) than PWS (mean = 58). Due to violations of sphericity [$X^2(2) = 7.13$; $p = 0.028$], degrees of freedom for the within subjects factor were corrected with Greenhouse-Geisser estimates [$\varepsilon = 0.868$]. There was no main effect of condition [$F(1.735,76.343) = 0.231$; $p = 0.763$] but a significant condition by group interaction [$F(1.735,76.343) = 4.899$; $p = 0.013$]. Independent samples *t*-tests revealed that the number of usable trials did not differ between groups in the SylC condition [$t(44) = 0.586$; $p = 0.561$], while TFS contributed more trials in the SylP [$t(44) = 2.902$; $p = 0.006$] and WordP [$t(44) = 3.286$; $p = 0.002$] conditions.

3.3. Mu cluster characteristics

Fig. 2 shows the distribution of components contributing to left and right μ clusters for both the PWS and matched controls. Of the 27 PWS

Table 1
Demographics and cluster contributions for PWS submitted to neural analysis.

Subject ID	Sex	Age	Handedness	μ component	Left included	Right included	SSI severity	Raw SSI
S1	M	31	R	L, R	2	1	very mild	16
S2	M	37	R	L	1		Mild	18
S3	M	24	R	L, R	1	1	Mild	24
S4	F	17	R	L, R	1	1	Very mild	13
S5	M	22	R	L	1		Very mild	16
S6	M	30	R	R		1	Very mild	12
S7	M	32	R	L, R	1	3	Very mild	16
S8	M	36	L	L, R	1	1	Mild	23
S9	F	18	R	L	1		Very mild	[1]
S10	M	22	R	L, R	1	1	Very mild	14
S11	M	26	L	L	1		[2]	
S12	F	17	R	L, R	3	3	Mild	21
S13	M	26	R	L, R	1	1	Mild	23
S14	M	22	R	R		2	Very mild	13
S15	M	18	R	R		2	Very mild	8
S16	M	32	R	L, R	2	2	Moderate	29
S17	M	18	R	L, R	1	1	Moderate	25
S18	F	23	R	L, R	2	1	Very mild	17
S19	F	18	R	R		1	Very mild	15
S20	M	18	R	L, R	4	1	Mild	24
S21	F	24	R	R		2	Very mild	11
S22	F	19	R	R		1	Very mild	12
S23	M	28	L	L, R	1	2	Very mild	17
S24	M	23	R	L, R	1	2	Moderate	30

1. Subject S9 had a diagnosis of persistent developmental stuttering, though did not produce any overt stuttering behaviors during SSI administration
2. Raw SSI Data were not available for Subject S11.
The 3 PWS omitted from this table produced μ components which could not be included in the analysis as they localized outside accepted μ rhythm generator sites (i.e., one to BA-7, one to BA-8, and another to BA-9).

Table 2
Demographics and cluster contributions for TFS submitted to neural analysis.

Subject ID	Sex	Age	Handedness	μ component	Left included	Right included
C1	M	37	R	R		2
C2	F	19	R	L, R		2
C3	M	26	R	L, R	1	2
C4	F	23	R	L	1	
C5	M	24	R	L, R	4	3
C6	F	19	R	L, R	3	3
C7	M	33	R	L, R	2	2
C8	F	28	R	L, R		2
C9	M	24	R	L, R	1	1
C10	M	38	R	R		
C11	M	44	R	L, R	1	
C12	F	22	R	L, R	2	3
C13	M	32	R	L, R	1	2
C14	F	18	R	L, R	2	2
C15	M	27	R	L, R	2	1
C16	M	22	R	L	1	
C17	M	18	R	L, R	1	1
C18	M	32	R	L, R	3	1
C19	M	20	R	L, R	2	3
C20	M	20	R	R		2
C21	M	34	L	L, R	2	1
C22	F	18	R	L, R		1
C23	M	28	R	L, R	1	1
C24	M	23	R	L, R	1	2

This table indicates the presence of a μ component in each hemisphere, as well as the number of components included in the between groups analysis to match the μ component contributions of PWS.

whose neural data were submitted to ICA/ERSP analysis, 24 (89%) produced either left or right μ components. Specifically, 17 produced bilateral μ components, 4 produced only left μ components, and 3 produced only right μ components. For the 24 matched controls recruited based on PWS μ component distribution, 24 (100%) produced either left or right μ components. Specifically, 19 produced bilateral μ components, 2 produced only left μ components, and 3 produced only right μ components. To ensure validity of the statistical comparison, cluster membership was constrained to matched pairs. That is, if either member of the matched pair did not produce a component contributing to a cluster, data from both subjects were excluded from the cluster.

3.3.1. Left mu

Data from 18 matched pairs were included in the left μ cluster. The total number of left μ components contributed by PWS was 26, while 31 components were contributed by their matched controls. The average ECD location for the left μ cluster was at Talairach [−34, −8, 43] (BA-6), with an unexplained RV of 8.11%. Cluster CSD maxima computed with sLORETA were localized to Talairach [−40, −15, 50] (BA-4). The Euclidean distance between the two source estimates is 1 cm.

3.3.2. Right mu

Data from 20 matched pairs were included in the right μ cluster. The total number of right μ components contributed by PWS was 30, while 37 components were contributed by their matched controls. The average ECD location for the right μ cluster was at Talairach [33, −7, 46] (BA-6), with an unexplained RV of 8.82%. Cluster CSD maxima computed with sLORETA were localized to Talairach [35, −10, 50] (BA-6). The Euclidean distance between the two source estimates was 0.53 cm.

3.3.3. EMG channel component correlations

The average r-values for the correlations between the time domain signal from the peri-labial EMG channel and the selected peri-labial EMG component resulting from ICA decomposition was 0.96 (SD = 0.04) for TFS and 0.95 (SD = 0.07) for PWS. The strength of correlation did not differ between groups [$t(46) = 0.46$, $p = 0.65$].

3.4. Between group ERSP differences

Figs. 3 and 4 show Van Essen cortical maps (computed with sLORETA) of significantly activated voxels ($p < 0.001$) contributing to left and right μ clusters, respectively. Van Essen maps are paired with

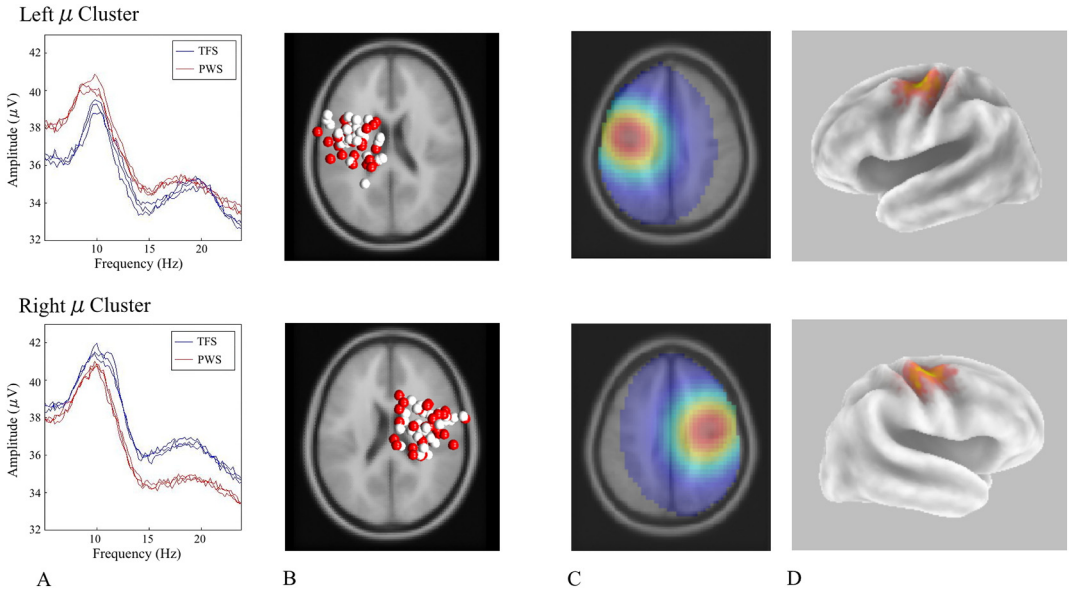

Fig. 2. Results for left and right μ clusters. (A) Mean spectra for cluster components. (B) ECD localizations for components contribution to μ clusters (TFS are white, PWS are red). (C) Probabilistic dipole density, illustrating maximal ECD cluster localization. (D) CSD μ cluster localization overlaid on Van Essen cortical model. Voxels active are significant at $p < 0.001$ (cluster corrections for multiple comparisons). (For interpretation of the references to color in this figure legend, the reader is referred to the web version of this article.)

ERSP analyses from each experimental condition for both groups across a range of 5–30 Hz. Significant between group differences ($p < 0.05$, cluster corrected) are displayed for each condition.

For the left μ cluster (Fig. 3), ERSP activity for both groups was characterized by μ ERD. In the SylC condition, PWS exhibited reduced ERD in both μ-α and μ-β bands approximately 500 ms following the production cue, and persisting through the remainder of the trial epoch. ERS differences (stronger in PWS) were also found in the non-relevant spectral valley (Fig. 2) between the bands of interest. In the WordP condition, PWS exhibited reduced ERD in both μ-α and μ-β bands approximately 500 ms following the cue to produce speech, persisting through the remainder of the trial epoch. No significant between group differences were noted in the SylP conditions.

For the right μ cluster (Fig. 4), ERSP activity for both groups was characterized by μ-α and μ-β ERD. No significant between group differences were found in any experimental condition.

3.4.1. EMG

Fig. 5 demonstrates peri-labial EMG activity across all experimental conditions for both groups. Peri-labial EMG activity was absent in the covert (SylC) production condition. EMG activity was characterized by ERS spreading across the frequency range, though strongest in the low frequencies. For both PWS and matched controls, EMG activity began following the cue to speak in the overt production conditions (SylP, WordP), and peaked approximately 500 ms later. No between group differences were found in any experimental condition.

3.5. Behavioral correlations

Correlation coefficients between SSI severity and mean time-frequency power across voxels demonstrating group differences were weak and non-significant ($r = -0.04$ in SylC and $r = 0.29$ in WordP).

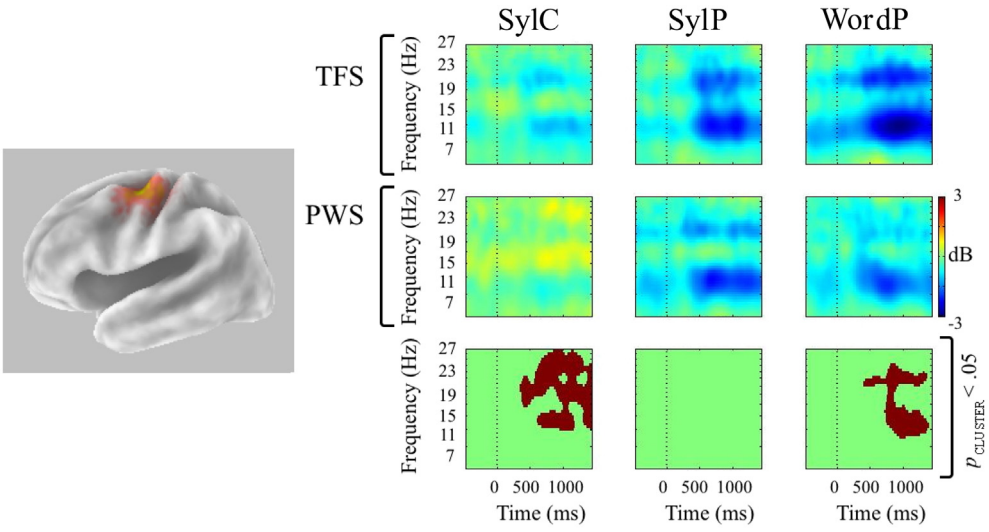

Fig. 3. The first column depicts the sLORETA CSD localization for the left μ cluster. The three columns to the right show ERSP analyses in SylC, SylP, and WordP conditions for both groups. The bottom row shows significant group differences at $p < 0.05$ (cluster corrections for multiple comparisons).

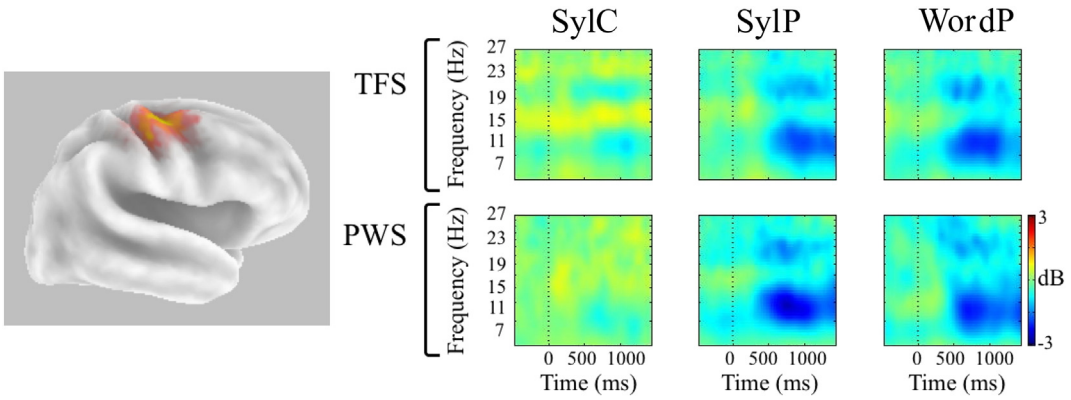

Fig. 4. The first column depicts the sLORETA CSD localization for the right μ cluster. The three columns to the right show ERSP analyses in SylC, SylP, and WordP conditions for both groups. No statistical comparisons are shown as no significant group differences existed.

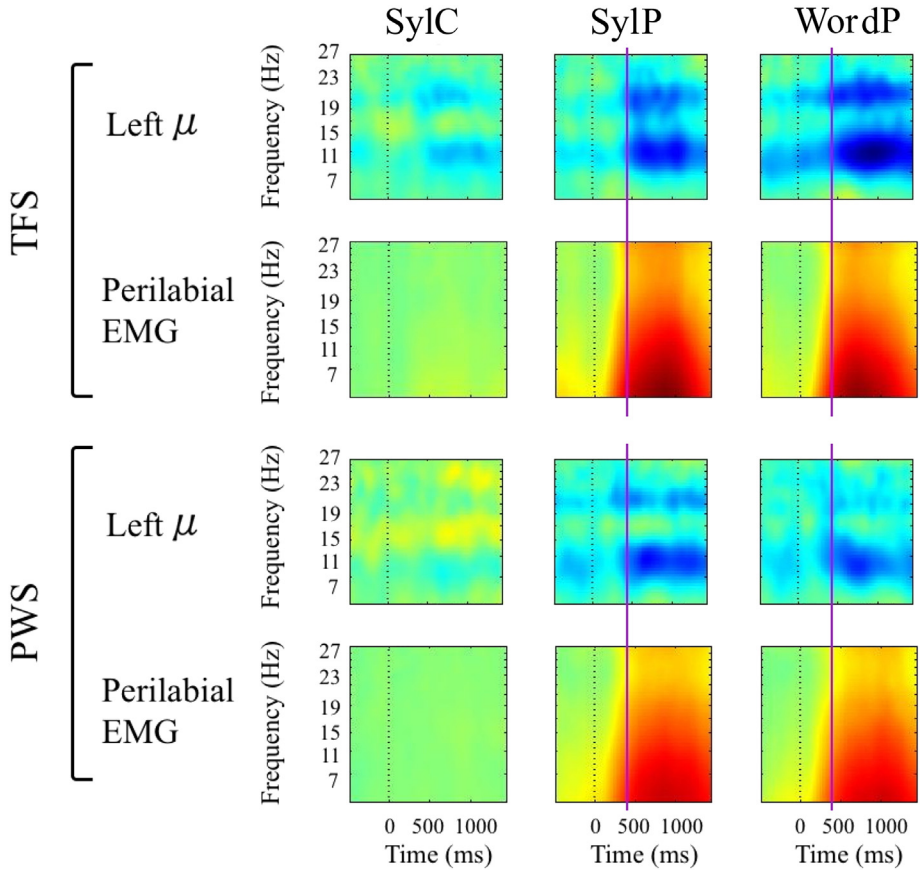

Fig. 5. ERSP analysis of left μ cluster overlaid in temporal synchrony with peri-labial EMG cluster activity for both groups. The dotted vertical line indicates the cue to initiate production, while the solid vertical line represents the onset of peak EMG activity during overt production conditions.

4. Discussion

ICA identified bilateral component clusters with characteristic μ spectra and RV < 20%. In line with other studies that have implemented similar cluster inclusion criteria, 89% of PWS and 100% of TFS contributed components to either left or right μ clusters (Nystrom, 2008; Bowers et al., 2013; Cuellar et al., 2016). μ clusters localized to BA-6 (precentral gyrus) in both left (Talairach [−40, −5, 50]) and right (Talairach [40, −5, 45]) hemispheres with activation spreading across anterior dorsal stream regions. Source localization is consistent with previous localizations of μ rhythm sources (Pineda, 2005; Hari, 2006; Bowers et al., 2013; Braadbaart et al., 2013) and expected sources of anterior dorsal stream activity (Hickok et al., 2011; Houde and Nagarajan, 2011; Guenther and Vladusich, 2012). ERSP analysis of μ cluster activity during spontaneous fluency is expected therefore to reliably reveal patterns of neural activity representing forward and inverse modeling across the time course of speech events.

Identification and temporal decomposition of neural and peri-labial EMG activity provides a novel means of investigating trait related neural differences in PWS. In both groups, EMG activity in the overt production tasks began with the cue to initiate speech. This suggests that subjects were preparing to speak during visual stimulus presentation and ready to speak when cued. Of critical relevance to the investigation of trait related differences in PWS, no group differences were found in either the strength or timing of EMG activity in overt production (Fig. 5). This suggests that muscle activity was similar for

both groups and that the methods employed to identify and exclude stuttered utterances were successful. As such, group differences in μ rhythm activity are interpreted as representing the trait-related sensorimotor differences associated with being a person who stutters, rather than state-related differences attributed to the presence of stuttering. Further evidence of trait-related differences are observed in the covert production tasks, free from motor influences.

4.1. Left hemisphere differences during overt production

The first hypothesis that PWS would demonstrate reduced μ-β ERD during overt production was supported by left hemisphere data from the WordP condition. In accord with previous μ rhythm studies describing oscillatory activity across speech production (Jenson et al., 2014, 2015), μ activity in TFS was characterized by weak μ-α and μ-β ERD preceding the cue to speak, followed by robust μ-α and μ-β ERD following the cue to speak that continued across the trial epoch (Fig. 3). In contrast, μ activity in PWS was marked by reduced μ-β ERD beginning with the cue to speak and persisting across utterances. As μ-β ERD typically marks the activation of forward models, reduced μ-β ERD in PWS during spontaneous fluency is interpreted as a trait-related weakness in forward modeling for speech (Max et al., 2004a, 2004b). The finding also is consistent with those of a meta-analysis of production based PET and fMRI studies in PWS (Belyk et al., 2015), which interpreted a reduced likelihood of left hemisphere anterior motor activation as a trait-related neural marker of stuttering. Further investigation of this trait-based weakness is necessary, however, as it remains unclear what characterizes a weak forward model (i.e., weak generation, weak transmission, or sparse parameter specification). Though the current EEG approach does not afford the spatial resolution of fMRI or PET, the precise temporal resolution offers a novel view of stuttering-related sensorimotor deficits. Specifically, reduced μ-β ERD was observed across the utterance, demonstrating that the fluent speech of PWS is characteristically unstable and therefore, prone to breakdown.

The absence of left hemisphere group differences during the ostensibly similar SylP conditions may have been driven by two primary effects. First, the syllables produced in the SylP condition were shorter than the tri-syllable nouns produced in the WordP condition. The reduced sequencing demands for shorter productions (Ghosh et al., 2008) may have led to reduced cortical activation (Riecker et al., 2008; Houde and Nagarajan, 2011). Second, syllable pairs are semantically neutral and may not activate the larger multimodal networks (Kotz et al., 2010) recruited by lexical items such as those used in WordP. The production of real words generates stronger neural responses than pseudo-words (Obleser and Weisz, 2012; Strauss et al., 2014). As a result, the reduced demands of the SylP task may have been insufficient to reveal differential patterns of internal modeling between the two groups.

The current findings of reduced μ-β ERD while speaking are in alignment with Belyk et al. (2015) as well as recent fNIRS (Walsh et al., 2017) and TMS/MEP (Neef et al., 2015) studies demonstrating reduced contributions of left hemisphere anterior sensorimotor regions in PWS. They also cohere, at least in part, with reports of reduced β activity in other disorders that affect the motor system including motor control impairments such as Parkinson's Disease (Delval et al., 2006; Degardin et al., 2009; Heinrichs-Graham et al., 2014; Moisello et al., 2015) and amyotrophic lateral sclerosis (Bizovicar et al., 2014). However, these findings contrast with those from a similar recent study by Mersov et al. (2016), who reported increased μ-β ERD in PWS during the preparation and overt production of sentences. They interpreted this as an elevated facilitatory signal to disinhibit a more strongly inhibited motor network secondary to basal ganglia thalamo-cortical loop dysfunction (Civier et al., 2013). Methodological differences between the Mersov et al. study and the current study, including the use of EEG vs. MEG, the inclusion of a carrier phrase, and the selection of a subject-specific word list based on probability of stuttering, may explain contrasting findings. It is important to note that both studies implicate μ-β oscillatory activity in trait-related deficits in PWS, and further investigation is warranted to clarify the contributions of forward modeling and timing network deficits.

The current study was performed with an adult cohort and it is possible the reduced μ-β ERD observed in PWS represents a long-standing adaptive strategy for motor control rather than a causal feature of the disorder. Over the course of a lifetime of stuttering, the brains of PWS may have identified that the forward model predictions are intermittently unreliable. The human brain can alter the relative weights assigned to different sensory modalities based on their degree of uncertainty (Oie et al., 2002; Klein et al., 2011), suggesting a capacity for adaptive weighting. Rather than the observed reduction in μ-β ERD representing a weakness in the forward model itself, it may instead represent a reduced weighting of forward model predictions secondary to their learned unreliability. Support for this proposal comes from evidence that the magnitude of μ-β oscillatory activity is dependent on confidence in forward model predictions (Tan et al., 2016), such that μ-β modulation is reduced when confidence in sensory predictions is low. Further studies implementing stable and unstable priming environments for speech production are necessary to determine if they elicit adaptive weighting of forward models.

Group differences in the μ-α band during the WordP condition also implicate a left hemisphere internal modeling deficit. TFS produced weak μ-α ERD prior to the cue to speak, followed by strong ERD concurrent with speech production. In contrast, PWS exhibited reduced μ-α ERD throughout the utterance. Considering interpretations of μ-α as a sensory feedback channel, data suggest a reduced contribution of the left hemisphere to sensorimotor feedback guidance for speech. This interpretation is consistent with reports of reduced pSTG activity in PWS during overt speech (Chang et al., 2009; Belyk et al., 2015), as well as interpretations of reduced μ-α ERD over anterior dorsal regions as evidence of sensorimotor dysfunction in clinical populations including Tourette's syndrome (Gunther et al., 1996) and Parkinson's disease (Brown and Marsden, 1999; Lim et al., 2006). Abnormal left hemisphere feedback control has been proposed by Hickok et al. (2011) also, who suggested that a noisy comparison between prediction and re-afference may underlie stuttering.

It should also be noted that within PWS, μ-α ERD appeared weaker than μ-β ERD in the WordP condition, suggesting a stronger contribution of sensory feedback processing to speech motor control. This interpretation is consistent with theoretical predictions arising from the DIVA model (Max et al., 2004a) and has been more recently supported through computational modeling (Civier et al., 2010). However, in order to disambiguate abnormal left hemisphere feedback contributions from somatosensory responses, it is necessary to consider how group differences emerge in covert speech.

4.2. Left hemisphere differences during covert production

The second hypothesis that PWS would demonstrate reduced μ-α and μ-β activity during covert speech was supported by the data from the left hemisphere (Fig. 3). In TFS, μ activity during covert syllable production was characterized by α and β ERD, though weaker in magnitude than the overt conditions. This weaker response to covert syllable production is consistent with previous reports (Gehrig et al., 2012; Jenson et al., 2014; Ylinen et al., 2015), and likely reflects the absence of primary motor and somatosensory responses not elicited during covert syllable production. Consideration of μ rhythm dynamics during covert syllable production thus enables evaluation of internal modeling without the influence of overt motor or somatosensory responses. Due to the absence of any behavioral marker for covert speech, it is possible that not all subjects covertly produced the syllable targets in every trial.

In contrast to the null findings from the overt syllable production tasks, group differences observed during covert syllable production

inform stuttering-related sensorimotor deficits. Activity in both μ-α and μ-β bands was significantly weaker in PWS than TFS. Given previous proposals that activity in the μ-α band represents sensory to motor feedback projections, the absence of μ-α ERD may suggest that little feedback was returned to PMC during covert production. In the absence of a reafferent signal, sensory feedback cannot be predicted via the internal loop to compensate for weak forward modeling (Hickok et al., 2011; Houde and Nagarajan, 2011; Tian and Poeppel, 2012), further exacerbating compromises to internal modeling. This sensorimotor loop breakdown during covert syllable production is in accord with reduced left hemisphere contributions to sensory feedback guidance in PWS. However, it remains unclear why in the current study group differences were detected in covert, but not overt, syllable production. Recall that in tasks requiring an overt response, μ oscillations capture primary motor and primary somatosensory activity in addition to sensorimotor activity. Therefore, it is possible that μ rhythm oscillations from covert speech tasks may be more sensitive to group differences as they only capture sensorimotor activity.

4.3. Non-significant differences of interest

Similarly to Walsh et al. (2017), no significant group differences were found between PWS and TFS in any condition in the right hemisphere. These findings are in contrast to previous reports of increased right hemisphere motor activity in PWS during speech (Fox et al., 1996, 2000; Brown et al., 2005; Loucks et al., 2011). While this may initially appear to undermine interpretations of right hemisphere compensation for the compromised left hemisphere (Preibisch et al., 2003; Neumann et al., 2005; Kell et al., 2009), it is critical to consider the relative contributions of left and right hemispheres to internal modeling for speech. Right hemisphere μ responses in TFS appeared weaker than left, though no such reduction was apparent in PWS. Data suggest a proportionally larger contribution of the right hemisphere to sensorimotor control of speech in PWS, aligning with Max et al.'s (2004a) assertion that PWS are overly reliant on external feedback, and reports that corrective feedback signals are mediated by the right hemisphere (Tourville and Guenther, 2011; Guenther and Vladusich, 2012). Further, this interpretation is consistent with reports that exogenous fluency enhancing conditions such as choral speech and delayed auditory feedback do not normalize right motor hyperactivity in PWS (Fox et al., 1996; Sakai et al., 2009) and elicit increased right motor activity in TFS (Watkins et al., 2008), though further work is necessary to clarify hemispheric contributions to sensorimotor control in PWS.

Though remarkably similar to those measured during speech perception (Saltuklaroglu et al., 2017) and resting state (Joos et al., 2014), reduced μ-β spectral power in the right hemisphere in PWS in the current study did not reach statistical significance. Group spectral differences may be important as they distinguish healthy controls from clinical populations such as individuals with dyslexia (Galin et al., 1992; Papagiannopoulou and Lagopoulos, 2016), insomnia (Buysse et al., 2008), epilepsy (Adebimpe et al., 2015), and Parkinson's (Caviness et al., 2016). Thus, further examination is warranted in an attempt to identify a neural biomarker for stuttering. The lack of significant correlations between raw SSI scores and μ power across voxels demonstrating group differences in both covert and overt speech tasks may have been due to the small degree of variability in stuttering severity in the subject cohort. Consequently, it remains unclear how the observed electrophysiologic differences give rise to the cluster of behaviors characteristic of the disorder.

5. General discussion

The temporal sensitivity of EEG was used to examine neural activity during spontaneously fluent overt and covert speech production in PWS and TFS to identify trait-related differences in internal modeling. Increased temporal and spectral precision afforded by the current methodology supplement hemodynamic imaging techniques by delineating forward modeling and sensory feedback responses across the time course of an utterance. The use of covert tasks enabled the probing of sensorimotor dynamics in the absence of the primary motor, somatosensory and auditory responses associated with overt speech. Consequently, reduced left hemisphere μ-β ERD in PWS is considered evidence of weak forward modeling, with reduced μ-α ERD representing reduced processing of sensory feedback. The presence of similar, albeit weaker, patterns of μ-α and μ-β ERD in covert speech, with the pattern of group differences unchanged, suggests two things. First, neither disfluency, nor even overt speech, is necessary to observe the trait-related sensorimotor impairment in PWS. Second, the availability of afferent feedback is insufficient to compensate for weak forward modeling in PWS and its persistent weakness across the time course of spontaneous fluency potentially represents a source of instability that predisposes even the fluent speech of PWS to breakdown.

μ-β activity also is sensitive to manipulations in timing (Fujioka et al., 2010, 2012, 2015), and has been interpreted as evidence of activity within basal ganglia loops (Bartolo and Merchant, 2015), as motor cortex is the site of integration for two main basal ganglia loops in motor control (Band and Van Boxtel, 1999; Dillon and Pizzagalli, 2007). Stuttering is well-known to be associated with basal ganglia dyfunction (Alm, 2004; Smits-Bandstra and De Nil, 2007; Chang and Zhu, 2013; Civier et al., 2013; Vanhoutte et al., 2016) and recent work has implicated μ-β oscillatory differences in stuttering populations to be indicative of coordination, timing, and sequencing of motor deficits during the production of normal rapid speech (Etchell et al., 2014, 2016). As the current study was not designed to vary timing, results were interpreted through the more traditional associations of μ rhythms. However, as sensorimotor control is under basal ganglia influence (Redgrave et al., 2010), future studies sensitive to changes in speech timing are necessary to delineate the contributions of sensorimotor and basal ganglia loops to the observed trait-related differences in μ-β activity.

The μ-α ERD observed during overt speech in both groups was interpreted as an index of sensory feedback projections (Tamura et al., 2012; Pineda et al., 2013; Quandt et al., 2013), highlighting the essential contribution of feedback control to internal modeling for speech espoused by SFC. The precise response profile of the μ-α band, however, remains unclear. Based on a posterior-to-anterior pattern of emergence, it has been proposed that μ-α represents an inverse internal model sent from posterior sensory regions to anterior dorsal regions (Sebastiani et al., 2014), though such an interpretation is not warranted by the findings of the current study. Connectivity measures, demonstrating information flow from sensory cortices to anterior motor regions in the μ-α band are necessary to expand current sensory feedback interpretations of μ-α to include inverse modeling. Current findings in both α and β bands of the μ rhythm are consistent with the theoretical predictions of SFC, and support its implementation as an overarching paradigm for the investigation of sensorimotor speech disorders. Further, the results of the current study validate the use of time-frequency decomposition of cooperative α and β channels of the unified μ rhythm to probe the roles of sensory feedback guidance and forward modeling, respectively, to other sensorimotor speech disorders.

6. Caveats

While the current study leveraged the temporal precision of EEG with the intermittent nature of stuttering to identify trait-based differences in sensorimotor control during spontaneous fluency, some limitations should be addressed. First, it must be acknowledged that a binary fluent/stuttered classification scheme may be overly simplified, especially considering reports that motor control occurs along a spectrum with even the fluent speech of PWS affected by underlying speech motor instabilities (Smith and Weber, 2017). Although the peri-labial EMG signal did not demonstrate group differences, the fluent speech of

PWS may still be acoustically and kinematically different from that of TFS (Smith and Kleinow, 2000) due to underlying deficits in and compensations to motor control. Additionally, these influences may be more present in an adult cohort (Armson and Kalinowski, 1994), potentially due to adaptation across a lifetime of stuttering. Thus, while the results of the current study were interpreted within the state-trait framework of Belyk et al. (2015), it must be acknowledged that this may be an imperfect dichotomy.

Second, while all subjects produced μ-like components, strict adherence to our inclusion criteria (i.e., μ spectra, RV% < 20%, localization to BA-1, -2, -3, -4, -6) meant that data from only 89% of subjects could be reliably assigned to μ clusters, with only 60% contributing to both clusters. Reduced subject contribution is a commonly reported finding in EEG research (Nystrom, 2008; Bowers et al., 2013; Jenson et al., 2014), and in the current study may have been driven by the use of a standard head model, as inclusion criteria are sensitive to individual anatomic variation. Reduced subject contribution would be expected to reduce statistical power leading to a Type 2 error, which speaks to the robust nature of the group differences identified in the present study.

Lastly, because covert speech production tasks do not require a behavioral response, it is not always clear that subjects are following instructions. Consequently, only one covert task was included in the current study. However, based on the discrepant findings between covert and overt syllable production, and overt syllable and overt word production, it is clear that inclusion of a covert word production task would have helped clarify the observed findings.

7. Conclusions and future directions

The novel technique of referencing EEG sensorimotor μ activity to peri-labial EMG activity during spontaneously fluent overt and covert speech facilitated identification of trait-related internal modeling deficits in PWS across the time course of speech production. Specifically, weak μ-α and μ-β ERD in both overt and covert production in PWS were considered evidence of reduced left hemisphere contributions to forward modeling and sensory feedback guidance for speech (Max et al., 2004a, 2004b). These results are consistent with abnormal projections from anterior motor to posterior sensory regions in PWS, therefore reducing effectiveness of forward modeling during speech. Future studies should investigate group differences in posterior dorsal stream regions, as well as connectivity measures across the sensorimotor speech network. The cost-effective and non-invasive nature of the methodology employed in the current study support its use examining neural activity in children who stutter to ascertain whether the trait-based differences revealed in the current study are causal to the stuttering pathology, or represent a cortical adaptation due to a lifetime of stuttering. Finally, using temporally precise measures to model the normalization of sensorimotor speech network dynamics during fluency enhancing conditions will enhance understanding of how the brains of PWS are able to modulate μ-α and μ-β band activity to overcome these trait-based forward modeling deficits. This increased understanding has the potential to give rise to more targeted therapeutic techniques (e.g., oscillatory-based neurofeedback (Sterman and Egner, 2006; Friedrich et al., 2015)) to minimize negative quality of life influences of stuttering.

Conflict of interest

The authors declare that they have no financial or non-financial relationships to disclose.

References

Adebimpe, A., Aarabi, A., Bourel-Ponchel, E., Mahmoudzadeh, M., Wallois, F., 2015. EEG resting state analysis of cortical sources in patients with benign epilepsy with centrotemporal spikes. Neuroimage Clin. 9, 275–282.

Alegre, M., Imirizaldu, L., Valencia, M., Iriarte, J., Arcocha, J., Artieda, J., 2006. Alpha and beta changes in cortical oscillatory activity in a go/no go randomly-delayed-response choice reaction time paradigm. Clin. Neurophysiol. 117, 16–25.

Alm, P.A., 2004. Stuttering and the basal ganglia circuits: a critical review of possible relations. J. Commun. Disord. 37, 325–369.

Armson, J., Kalinowski, J., 1994. Interpreting results of the fluent speech paradigm in stuttering research: difficulties in separating cause from effect. J. Speech Hear. Res. 37, 69–82.

Arnstein, D., Cui, F., Keysers, C., Maurits, N.M., Gazzola, V., 2011. Mu-suppression during action observation and execution correlates with BOLD in dorsal premotor, inferior parietal, and SI cortices. J. Neurosci. 31, 14243–14249.

Babiloni, C., Babiloni, F., Carducci, F., Cincotti, F., Cocozza, G., Del Percio, C., Moretti, D.V., Rossini, P.M., 2002. Human cortical electroencephalography (EEG) rhythms during the observation of simple aimless movements: a high-resolution EEG study. NeuroImage 17, 559–572.

Band, G.P., Van Boxtel, G.J., 1999. Inhibitory motor control in stop paradigms: review and reinterpretation of neural mechanisms. Acta Psychol. 101, 179–211.

Bartolo, R., Merchant, H., 2015. Beta oscillations are linked to the initiation of sensory-cued movement sequences and the internal guidance of regular tapping in the monkey. J. Neurosci. 35, 4635–4640.

Beal, D.S., Gracco, V.L., Lafaille, S.J., De Nil, L.F., 2007. Voxel-based morphometry of auditory and speech-related cortex in stutterers. Neuroreport 18, 1257–1260.

Beal, D.S., Cheyne, D.O., Gracco, V.L., Quraan, M.A., Taylor, M.J., De Nil, L.F., 2010. Auditory evoked fields to vocalization during passive listening and active generation in adults who stutter. NeuroImage 52, 1645–1653.

Beal, D.S., Quraan, M.A., Cheyne, D.O., Taylor, M.J., Gracco, V.L., De Nil, L.F., 2011. Speech-induced suppression of evoked auditory fields in children who stutter. NeuroImage 54, 2994–3003.

Beal, D.S., Gracco, V.L., Brettschneider, J., Kroll, R.M., De Nil, L.F., 2013. A voxel-based morphometry (VBM) analysis of regional grey and white matter volume abnormalities within the speech production network of children who stutter. Cortex 49, 2151–2161.

Belyk, M., Kraft, S.J., Brown, S., 2015. Stuttering as a trait or state - an ALE meta-analysis of neuroimaging studies. Eur. J. Neurosci. 41, 275–284.

Bizovicar, N., Dreo, J., Koritnik, B., Zidar, J., 2014. Decreased movement-related beta desynchronization and impaired post-movement beta rebound in amyotrophic lateral sclerosis. Clin. Neurophysiol. 125, 1689–1699.

Blockcolsky, V., Frazer, J., Frazer, D., 2008. 40,000 Selected Words. Communiation Skill Builders, San Antonio, TX.

Bowers, A., Saltuklaroglu, T., Harkrider, A., Cuellar, M., 2013. Suppression of the micro rhythm during speech and non-speech discrimination revealed by independent component analysis: implications for sensorimotor integration in speech processing. PLoS One 8, e72024.

Braadbaart, L., Williams, J.H., Waiter, G.D., 2013. Do mirror neuron areas mediate mu rhythm suppression during imitation and action observation? Int. J. Psychophysiol. 89, 99–105.

Braun, A.R., Varga, M., Stager, S., Schulz, G., Selbie, S., Maisog, J.M., Carson, R.E., Ludlow, C.L., 1997. Altered patterns of cerebral activity during speech and language production in developmental stuttering. An H2(15)O positron emission tomography study. Brain 120 (Pt 5), 761–784.

Brinkman, L., Stolk, A., Dijkerman, H.C., De Lange, F.P., Toni, I., 2014. Distinct roles for alpha- and beta-band oscillations during mental simulation of goal-directed actions. J. Neurosci. 34, 14783–14792.

Brown, S.F., 1945. The loci of stutterings in the speech sequence. J. Speech Disord. 10, 181–192.

Brown, P., Marsden, C.D., 1999. Bradykinesia and impairment of EEG desynchronization in Parkinson's disease. Mov. Disord. 14, 423–429.

Brown, S., Ingham, R.J., Ingham, J.C., Laird, A.R., Fox, P.T., 2005. Stuttered and fluent speech production: an ALE meta-analysis of functional neuroimaging studies. Hum. Brain Mapp. 25, 105–117.

Brunner, C., Delorme, A., Makeig, S., 2013. Eeglab - an open source Matlab toolbox for electrophysiological research. Biomed Tech (Berl).

Buysse, D.J., Germain, A., Hall, M.L., Moul, D.E., Nofzinger, E.A., Begley, A., Ehlers, C.L., Thompson, W., Kupfer, D.J., 2008. EEG spectral analysis in primary insomnia: NREM period effects and sex differences. Sleep 31, 1673–1682.

Cai, S., Tourville, J.A., Beal, D.S., Perkell, J.S., Guenther, F.H., Ghosh, S.S., 2014. Diffusion imaging of cerebral white matter in persons who stutter: evidence for network-level anomalies. Front. Hum. Neurosci. 8, 54.

Caviness, J.N., Utianski, R.L., Hentz, J.G., Beach, T.G., Dugger, B.N., Shill, H.A., Driver-Dunckley, E.D., Sabbagh, M.N., Mehta, S., Adler, C.H., 2016. Differential spectral quantitative electroencephalography patterns between control and Parkinson's disease cohorts. Eur. J. Neurol. 23, 387–392.

Chang, S.E., 2014. Research updates in neuroimaging studies of children who stutter. Semin. Speech Lang. 35, 67–79.

Chang, S.E., Zhu, D.C., 2013. Neural network connectivity differences in children who stutter. Brain 136, 3709–3726.

Chang, S.E., Erickson, K.I., Ambrose, N.G., Hasegawa-Johnson, M.A., Ludlow, C.L., 2008. Brain anatomy differences in childhood stuttering. NeuroImage 39, 1333–1344.

Chang, S.E., Kenney, M.K., Loucks, T.M., Ludlow, C.L., 2009. Brain activation abnormalities during speech and non-speech in stuttering speakers. NeuroImage 46, 201–212.

Chang, S.E., Horwitz, B., Ostuni, J., Reynolds, R., Ludlow, C.L., 2011. Evidence of left inferior frontal-premotor structural and functional connectivity deficits in adults who stutter. Cereb. Cortex 21, 2507–2518.

Chatrian, G.E., Lettich, E., Nelson, P.L., 1988. Modified nomenclature for the “10%” electrode system. J. Clin. Neurophysiol. 5, 183–186.

Cieslak, M., Ingham, R.J., Ingham, J.C., Grafton, S.T., 2015. Anomalous white matter morphology in adults who stutter. J. Speech Lang. Hear. Res. 58, 268–277.
Civier, O., Tasko, S.M., Guenther, F.H., 2010. Overreliance on auditory feedback may lead to sound/syllable repetitions: simulations of stuttering and fluency-inducing conditions with a neural model of speech production. J. Fluen. Disord. 35, 246–279.
Civier, O., Bullock, D., Max, L., Guenther, F.H., 2013. Computational modeling of stuttering caused by impairments in a basal ganglia thalamo-cortical circuit involved in syllable selection and initiation. Brain Lang. 126, 263–278.
Connally, E.L., Ward, D., Howell, P., Watkins, K.E., 2014. Disrupted white matter in language and motor tracts in developmental stuttering. Brain Lang. 131, 25–35.
Crapse, T.B., Sommer, M.A., 2008. Corollary discharge across the animal kingdom. Nat. Rev. Neurosci. 9, 587–600.
Cuellar, M., Harkrider, A.W., Jenson, D., Thornton, D., Bowers, A., Saltuklaroglu, T., 2016. Time-frequency analysis of the EEG mu rhythm as a measure of sensorimotor integration in the later stages of swallowing. Clin. Neurophysiol. 127, 2625–2635.
Curio, G., Neuloh, G., Numminen, J., Jousmaki, V., Hari, R., 2000. Speaking modifies voice-evoked activity in the human auditory cortex. Hum. Brain Mapp. 9, 183–191.
Daliri, A., Max, L., 2015a. Electrophysiological evidence for a general auditory prediction deficit in adults who stutter. Brain Lang. 150, 37–44.
Daliri, A., Max, L., 2015b. Modulation of auditory processing during speech movement planning is limited in adults who stutter. Brain Lang. 143, 59–68.
Daliri, A., Max, L., 2016. Modulation of auditory responses to speech vs. nonspeech stimuli during speech movement planning. Front. Hum. Neurosci. 10, 234.
Daliri, A., Prokopenko, R.A., Flanagan, J.R., Max, L., 2014. Control and prediction components of movement planning in stuttering versus nonstuttering adults. J. Speech Lang. Hear. Res. 57, 2131–2141.
Degardin, A., Houdayer, E., Bourriez, J.L., Destee, A., Defebvre, L., Derambure, P., Devos, D., 2009. Deficient “sensory” beta synchronization in Parkinson's disease. Clin. Neurophysiol. 120, 636–642.
Delorme, A., Palmer, J., Onton, J., Oostenveld, R., Makeig, S., 2012. Independent EEG sources are dipolar. PLoS One 7, e30135.
Delval, A., Defebvre, L., Labyt, E., Douay, X., Bourriez, J.L., Waucquiez, N., Derambure, P., Destee, A., 2006. Movement-related cortical activation in familial Parkinson disease. Neurology 67, 1086–1087.
Di Nota, P.M., Chartrand, J.M., Levkov, G.R., Montefusco-Siegmund, R., Desouza, J.F., 2017. Experience-dependent modulation of alpha and beta during action observation and motor imagery. BMC Neurosci. 18, 28.
Dillon, D.G., Pizzagalli, D.A., 2007. Inhibition of action, thought, and emotion: a selective neurobiological review. Appl. Prev. Psychol. 12, 99–114.
Drayna, D., Kang, C., 2011. Genetic approaches to understanding the causes of stuttering. J. Neurodev. Disord. 3, 374–380.
Duann, J.-R., Chiou, J.-C., 2016. A comparison of independent event-related desynchronization responses in motor-related brain areas to movement execution, movement imagery, and movement observation. PLoS One 11, e0162546.
Dziewas, R., Soros, P., Ishii, R., Chau, W., Henningsen, H., Ringelstein, E.B., Knecht, S., Pantev, C., 2003. Neuroimaging evidence for cortical involvement in the preparation and in the act of swallowing. NeuroImage 20, 135–144.
Erbil, N., Ungan, P., 2007. Changes in the alpha and beta amplitudes of the central EEG during the onset, continuation, and offset of long-duration repetitive hand movements. Brain Res. 1169, 44–56.
Etchell, A.C., Johnson, B.W., Sowman, P.F., 2014. Beta oscillations, timing, and stuttering. Front. Hum. Neurosci. 8, 1036.
Etchell, A.C., Ryan, M., Martin, E., Johnson, B.W., Sowman, P.F., 2016. Abnormal time course of low beta modulation in non-fluent preschool children: a magnetoencephalographic study of rhythm tracking. NeuroImage 125, 953–963.
Falk, S., Muller, T., Dalla Bella, S., 2015. Non-verbal sensorimotor timing deficits in children and adolescents who stutter. Front. Psychol. 6, 847.
Foundas, A.L., Bollich, A.M., Corey, D.M., Hurley, M., Heilman, K.M., 2001. Anomalous anatomy of speech-language areas in adults with persistent developmental stuttering. Neurology 57, 207–215.
Fox, P.T., Ingham, R.J., Ingham, J.C., Hirsch, T.B., Downs, J.H., Martin, C., Jerabek, P., Glass, T., Lancaster, J.L., 1996. A PET study of the neural systems of stuttering. Nature 382, 158–161.
Fox, P.T., Ingham, R.J., Ingham, J.C., Zamarripa, F., Xiong, J.H., Lancaster, J.L., 2000. Brain correlates of stuttering and syllable production. A PET performance-correlation analysis. Brain 123 (Pt 10), 1985–2004.
Friedrich, E.V., Sivanathan, A., Lim, T., Suttie, N., Louchart, S., Pillen, S., Pineda, J.A., 2015. An effective neurofeedback intervention to improve social interactions in children with autism Spectrum disorder. J. Autism Dev. Disord. 45, 4084–4100.
Fujioka, T., Zendel, B.R., Ross, B., 2010. Endogenous neuromagnetic activity for mental hierarchy of timing. J. Neurosci. 30, 3458–3466.
Fujioka, T., Trainor, L.J., Large, E.W., Ross, B., 2012. Internalized timing of isochronous sounds is represented in neuromagnetic beta oscillations. J. Neurosci. 32, 1791–1802.
Fujioka, T., Ross, B., Trainor, L.J., 2015. Beta-band oscillations represent auditory beat and its metrical hierarchy in perception and imagery. J. Neurosci. 35, 15187–15198.
Galin, D., Raz, J., Fein, G., Johnstone, J., Herron, J., Yingling, C., 1992. EEG spectra in dyslexic and normal readers during oral and silent reading. Electroencephalogr. Clin. Neurophysiol. 82, 87–101.
Gehrig, J., Wibral, M., Arnold, C., Kell, C.A., 2012. Setting up the speech production network: how oscillations contribute to lateralized information routing. Front. Psychol. 3, 169.
Ghosh, S.S., Tourville, J.A., Guenther, F.H., 2008. A neuroimaging study of premotor lateralization and cerebellar involvement in the production of phonemes and syllables. J. Speech Lang. Hear. Res. 51, 1183–1202.
Giraud, A.L., Neumann, K., Bachoud-Levi, A.C., Von Gudenberg, A.W., Euler, H.A., Lanfermann, H., Preibisch, C., 2008. Severity of dysfluency correlates with basal ganglia activity in persistent developmental stuttering. Brain Lang. 104, 190–199.
Gracco, V.L., 1988. Timing factors in the coordination of speech movements. J. Neurosci. 8, 4628–4639.
Gramann, K., Gwin, J.T., Bigdely-Shamlo, N., Ferris, D.P., Makeig, S., 2010. Visual evoked responses during standing and walking. Front. Hum. Neurosci. 4, 202.
Guenther, F.H., Vladusich, T., 2012. A neural theory of speech acquisition and production. J. Neurolinguistics 25, 408–422.
Gunther, W., Muller, N., Trapp, W., Haag, C., Putz, A., Straube, A., 1996. Quantitative EEG analysis during motor function and music perception in Tourette's syndrome. Eur. Arch. Psychiatry Clin. Neurosci. 246, 197–202.
Hari, R., 2006. Action-perception connection and the cortical mu rhythm. Prog. Brain Res. 159, 253–260.
Heinrichs-Graham, E., Wilson, T.W., Santamaria, P.M., Heithoff, S.K., Torres-Russotto, D., Hutter-Saunders, J.A., Estes, K.A., Meza, J.L., Mosley, R.L., Gendelman, H.E., 2014. Neuromagnetic evidence of abnormal movement-related beta desynchronization in Parkinson's disease. Cereb. Cortex 24, 2669–2678.
Hickok, G., Poeppel, D., 2004. Dorsal and ventral streams: a framework for understanding aspects of the functional anatomy of language. Cognition 92, 67–99.
Hickok, G., Poeppel, D., 2007. The cortical organization of speech processing. Nat. Rev. Neurosci. 8, 393–402.
Hickok, G., Houde, J., Rong, F., 2011. Sensorimotor integration in speech processing: computational basis and neural organization. Neuron 69, 407–422.
Houde, J.F., Nagarajan, S.S., 2011. Speech production as state feedback control. Front. Hum. Neurosci. 5, 82.
Howell, P., Jiang, J., Peng, D., Lu, C., 2012. Neural control of rising and falling tones in Mandarin speakers who stutter. Brain Lang. 123, 211–221.
Ingham, R.J., Fox, P.T., Costello Ingham, J., Zamarripa, F., 2000. Is overt stuttered speech a prerequisite for the neural activations associated with chronic developmental stuttering? Brain Lang. 75, 163–194.
Ingham, R.J., Grafton, S.T., Bothe, A.K., Ingham, J.C., 2012. Brain activity in adults who stutter: similarities across speaking tasks and correlations with stuttering frequency and speaking rate. Brain Lang. 122, 11–24.
Jasper, H.H., 1958. The ten twenty electrode system of the international federation. Electroencephalogr. Clin. Neurophysiol. 10, 371–375.
Jenson, D., Bowers, A.L., Harkrider, A.W., Thornton, D., Cuellar, M., Saltuklaroglu, T., 2014. Temporal dynamics of sensorimotor integration in speech perception and production: independent component analysis of EEG data. Front. Psychol. 5, 656.
Jenson, D., Harkrider, A.W., Thornton, D., Bowers, A.L., Saltuklaroglu, T., 2015. Auditory cortical deactivation during speech production and following speech perception: an EEG investigation of the temporal dynamics of the auditory alpha rhythm. Front. Hum. Neurosci. 9, 534.
Jones, S.R., Pritchett, D.L., Sikora, M.A., Stufflebeam, S.M., Hamalainen, M., Moore, C.I., 2009. Quantitative analysis and biophysically realistic neural modeling of the MEG mu rhythm: rhythmogenesis and modulation of sensory-evoked responses. J. Neurophysiol. 102, 3554–3572.
Joos, K., De Ridder, D., Boey, R.A., Vanneste, S., 2014. Functional connectivity changes in adults with developmental stuttering: a preliminary study using quantitative electroencephalography. Front. Hum. Neurosci. 8, 783.
Kell, C.A., Neumann, K., Von Kriegstein, K., Posenenske, C., Von Gudenberg, A.W., Euler, H., Giraud, A.L., 2009. How the brain repairs stuttering. Brain 132, 2747–2760.
Kilavik, B.E., Zaepffel, M., Brovelli, A., MacKay, W.A., Riehle, A., 2013. The ups and downs of beta oscillations in sensorimotor cortex. Exp. Neurol. 245, 15–26.
Klein, T.J., Jeka, J., Kiemel, T., Lewis, M.A., 2011. Navigating sensory conflict in dynamic environments using adaptive state estimation. Biol. Cybern. 105, 291–304.
Kotz, S.A., D'ausilio, A., Raettig, T., Begliomini, C., Craighero, L., Fabbri-Destro, M., Zingales, C., Haggard, P., Fadiga, L., 2010. Lexicality drives audio-motor transformations in Broca's area. Brain Lang. 112, 3–11.
Lee, T.W., Girolami, M., Sejnowski, T.J., 1999. Independent component analysis using an extended infomax algorithm for mixed subgaussian and supergaussian sources. Neural Comput. 11, 417–441.
Lim, V.K., Hamm, J.P., Byblow, W.D., Kirk, I.J., 2006. Decreased desychronisation during self-paced movements in frequency bands involving sensorimotor integration and motor functioning in Parkinson's disease. Brain Res. Bull. 71, 245–251.
Loucks, T., Kraft, S.J., Choo, A.L., Sharma, H., Ambrose, N.G., 2011. Functional brain activation differences in stuttering identified with a rapid fMRI sequence. J. Fluen. Disord. 36, 302–307.
Makeig, S., Debener, S., Onton, J., Delorme, A., 2004. Mining event-related brain dynamics. Trends Cogn. Sci. 8, 204–210.
Maris, E., Oostenveld, R., 2007. Nonparametric statistical testing of EEG- and MEG-data. J. Neurosci. Methods 164, 177–190.
Max, L., Guenther, F.H., Gracco, V.L., Ghosh, S.S., Wallace, M.E., 2004a. Unstable or insufficiently activated internal models and feedback-biased motor control as sources of dysfluency: a theoretical model of stuttering. In: Contemporary Issues in Communication Science and Disorders. 31. pp. 105–122.
Max, L., Maassen, B., Kent, R., Peters, H., Van Lieshout, P., Hulstijin, W., 2004b. Stuttering and internal models for sensorimotor control: a theoretical perspective to generate testable hypotheses. In: Speech Motor Control in Normal and Disordered Speech, pp. 357–387.
Mazziotta, J., Toga, A., Evans, A., Fox, P., Lancaster, J., Zilles, K., Woods, R., Paus, T., Simpson, G., Pike, B., Holmes, C., Collins, L., Thompson, P., MacDonald, D., Iacoboni, M., Schormann, T., Amunts, K., Palomero-Gallagher, N., Geyer, S., Parsons, L., Narr, K., Kabani, N., Le Goualher, G., Boomsma, D., Cannon, T., Kawashima, R., Mazoyer, B., 2001. A probabilistic atlas and reference system for the human brain: International Consortium for Brain Mapping (ICBM). Philos. Trans. R. Soc. Lond. Ser. B Biol. Sci. 356, 1293–1322.
Mersov, A.M., Jobst, C., Cheyne, D.O., De Nil, L., 2016. Sensorimotor oscillations prior to

speech onset reflect altered motor networks in adults who stutter. Front. Hum. Neurosci. 10, 443.
Moisello, C., Blanco, D., Lin, J., Panday, P., Kelly, S.P., Quartarone, A., Di Rocco, A., Cirelli, C., Tononi, G., Ghilardi, M.F., 2015. Practice changes beta power at rest and its modulation during movement in healthy subjects but not in patients with Parkinson's disease. Brain Behav. 5, e00374.
Muthukumaraswamy, S.D., Johnson, B.W., 2004. Changes in rolandic mu rhythm during observation of a precision grip. Psychophysiology 41, 152–156.
Nakayashiki, K., Saeki, M., Takata, Y., Hayashi, Y., Kondo, T., 2014. Modulation of event-related desynchronization during kinematic and kinetic hand movements. J. Neuroeng. Rehabil. 11, 1.
Namasivayam, A.K., Van Lieshout, P., Mcilroy, W.E., De Nil, L., 2009. Sensory feedback dependence hypothesis in persons who stutter. Hum. Mov. Sci. 28, 688–707.
Neef, N.E., Hoang, T.N., Neef, A., Paulus, W., Sommer, M., 2015. Speech dynamics are coded in the left motor cortex in fluent speakers but not in adults who stutter. Brain 138, 712–725.
Neumann, K., Euler, H.A., Von Gudenberg, A.W., Giraud, A.L., Lanfermann, H., Gall, V., Preibisch, C., 2003. The nature and treatment of stuttering as revealed by fMRI a within- and between-group comparison. J. Fluen. Disord. 28, 381–409 (quiz 409-410).
Neumann, K., Preibisch, C., Euler, H.A., Von Gudenberg, A.W., Lanfermann, H., Gall, V., Giraud, A.L., 2005. Cortical plasticity associated with stuttering therapy. J. Fluen. Disord. 30, 23–39.
Niziolek, C.A., Nagarajan, S.S., Houde, J.F., 2013. What does motor efference copy represent? Evidence from speech production. J. Neurosci. 33, 16110–16116.
Numminen, J., Salmelin, R., Hari, R., 1999. Subject's own speech reduces reactivity of the human auditory cortex. Neurosci. Lett. 265, 119–122.
Nystrom, P., 2008. The infant mirror neuron system studied with high density EEG. Soc. Neurosci. 3, 334–347.
Oberman, L.M., Hubbard, E.M., McCleery, J.P., Altschuler, E.L., Ramachandran, V.S., Pineda, J.A., 2005. EEG evidence for mirror neuron dysfunction in autism spectrum disorders. Brain Res. Cogn. Brain Res. 24, 190–198.
Obleser, J., Weisz, N., 2012. Suppressed alpha oscillations predict intelligibility of speech and its acoustic details. Cereb. Cortex 22, 2466–2477.
Oie, K.S., Kiemel, T., Jeka, J.J., 2002. Multisensory fusion: simultaneous re-weighting of vision and touch for the control of human posture. Brain Res. Cogn. Brain Res. 14, 164–176.
Oldfield, R.C., 1971. The assessment and analysis of handedness: the Edinburgh inventory. Neuropsychologia 9, 97–113.
Onton, J., Westerfield, M., Townsend, J., Makeig, S., 2006. Imaging human EEG dynamics using independent component analysis. Neurosci. Biobehav. Rev. 30, 808–822.
Oostenveld, R., Oostendorp, T.F., 2002. Validating the boundary element method for forward and inverse EEG computations in the presence of a hole in the skull. Hum. Brain Mapp. 17, 179–192.
Papagiannopoulou, E.A., Lagopoulos, J., 2016. Resting state EEG hemispheric power asymmetry in children with dyslexia. Front Pediatr. 4, 11.
Pascual-Marqui, R.D., 2002. Standardized low-resolution brain electromagnetic tomography (sLORETA): technical details. Methods Find. Exp. Clin. Pharmacol. 24 (Suppl. D), 5–12.
Pineda, J.A., 2005. The functional significance of mu rhythms: translating “seeing” and “hearing” into “doing”. Brain Res. Brain Res. Rev. 50, 57–68.
Pineda, J.A., Grichanik, M., Williams, V., Trieu, M., Chang, H., Keysers, C., 2013. EEG sensorimotor correlates of translating sounds into actions. Front. Neurosci. 7, 203.
Pistohl, T., Schulze-Bonhage, A., Aertsen, A., Mehring, C., Ball, T., 2012. Decoding natural grasp types from human ECoG. NeuroImage 59, 248–260.
Preibisch, C., Neumann, K., Raab, P., Euler, H.A., Von Gudenberg, A.W., Lanfermann, H., Giraud, A.L., 2003. Evidence for compensation for stuttering by the right frontal operculum. NeuroImage 20, 1356–1364.
Quandt, L.C., Marshall, P.J., Bouquet, C.A., Shipley, T.F., 2013. Somatosensory experiences with action modulate alpha and beta power during subsequent action observation. Brain Res. 1534, 55–65.
Redgrave, P., Rodriguez, M., Smith, Y., Rodriguez-Oroz, M.C., Lehericy, S., Bergman, H., Agid, Y., Delong, M.R., Obeso, J.A., 2010. Goal-directed and habitual control in the basal ganglia: implications for Parkinson's disease. Nat. Rev. Neurosci. 11, 760–772.
Rektor, I., Sochůrková, D., Bočková, M., 2006. Intracerebral ERD/ERS in voluntary movement and in cognitive visuomotor task. Prog. Brain Res. 159, 311–330.
Richards, J.E., 2004. Recovering dipole sources from scalp-recorded event-related-potentials using component analysis: principal component analysis and independent component analysis. Int. J. Psychophysiol. 54, 201–220.
Riecker, A., Brendel, B., Ziegler, W., Erb, M., Ackermann, H., 2008. The influence of syllable onset complexity and syllable frequency on speech motor control. Brain Lang. 107, 102–113.
Riley, G., 2009. The Stuttering Severity Instrument for Adults and Children (SSI-4). PRO-ED, Austin, TX.
Sabate, M., Llanos, C., Enriquez, E., Rodriguez, M., 2012. Mu rhythm, visual processing and motor control. Clin. Neurophysiol. 123, 550–557.
Sakai, N., Masuda, S., Shimotomai, T., Mori, K., 2009. Brain activation in adults who stutter under delayed auditory feedback: an fMRI study. Int. J. Speech Lang. Pathol. 11, 2–11.
Saltuklaroglu, T., Kalinowski, J., 2011. The inhibition of stuttering via the perceptions and production of syllable repetitions. Int. J. Neurosci. 121, 44–49.
Saltuklaroglu, T., Harkrider, A.W., Thornton, D., Jenson, D., Kittilstved, T., 2017. EEG mu (micro) rhythm spectra and oscillatory activity differentiate stuttering from non-stuttering adults. NeuroImage 153, 232–245.
Sebastiani, V., De Pasquale, F., Costantini, M., Mantini, D., Pizzella, V., Romani, G.L., Della Penna, S., 2014. Being an agent or an observer: different spectral dynamics revealed by MEG. NeuroImage 102 (Pt 2), 717–728.
Seeber, M., Scherer, R., Wagner, J., Solis-Escalante, T., Muller-Putz, G.R., 2014. EEG beta suppression and low gamma modulation are different elements of human upright walking. Front. Hum. Neurosci. 8, 485.
Smith, A., Kleinow, J., 2000. Kinematic correlates of speaking rate changes in stuttering and normally fluent adults. J. Speech Lang. Hear. Res. 43, 521–536.
Smith, A., Weber, C., 2017. How stuttering develops: the multifactorial dynamic pathways theory. J. Speech Lang. Hear. Res. 60, 2483–2505.
Smits-Bandstra, S., De Nil, L.F., 2007. Sequence skill learning in persons who stutter: implications for cortico-striato-thalamo-cortical dysfunction. J. Fluen. Disord. 32, 251–278.
Sommer, M., Koch, M.A., Paulus, W., Weiller, C., Buchel, C., 2002. Disconnection of speech-relevant brain areas in persistent developmental stuttering. Lancet 360, 380–383.
Stancak Jr., A., Riml, A., Pfurtscheller, G., 1997. The effects of external load on movement-related changes of the sensorimotor EEG rhythms. Electroencephalogr. Clin. Neurophysiol. 102, 495–504.
Sterman, M.B., Egner, T., 2006. Foundation and practice of neurofeedback for the treatment of epilepsy. Appl. Psychophysiol. Biofeedback 31, 21.
Stone, J.V., 2004. Independent Component Analysis. Wiley Online Library.
Strauss, A., Kotz, S.A., Scharinger, M., Obleser, J., 2014. Alpha and theta brain oscillations index dissociable processes in spoken word recognition. NeuroImage 97, 387–395.
Suresh, R., Ambrose, N., Roe, C., Pluzhnikov, A., Wittke-Thompson, J.K., Ng, M.C., Wu, X., Cook, E.H., Lundstrom, C., Garsten, M., Ezrati, R., Yairi, E., Cox, N.J., 2006. New complexities in the genetics of stuttering: significant sex-specific linkage signals. Am. J. Hum. Genet. 78, 554–563.
Tamura, T., Gunji, A., Takeichi, H., Shigemasu, H., Inagaki, M., Kaga, M., Kitazaki, M., 2012. Audio-vocal monitoring system revealed by mu-rhythm activity. Front. Psychol. 3, 225.
Tan, H., Jenkinson, N., Brown, P., 2014. Dynamic neural correlates of motor error monitoring and adaptation during trial-to-trial learning. J. Neurosci. 34, 5678–5688.
Tan, H., Wade, C., Brown, P., 2016. Post-movement Beta activity in sensorimotor cortex indexes confidence in the estimations from internal models. J. Neurosci. 36, 1516–1528.
Thornton, D., Harkrider, A.W., Jenson, D., Saltuklaroglu, T., 2017. Sensorimotor activity measured via oscillations of EEG mu rhythms in speech and non-speech discrimination tasks with and without segmentation requirements. Brain Lang.
Tian, X., Poeppel, D., 2010. Mental imagery of speech and movement implicates the dynamics of internal forward models. Front. Psychol. 1, 166.
Tian, X., Poeppel, D., 2012. Mental imagery of speech: linking motor and perceptual systems through internal simulation and estimation. Front. Hum. Neurosci. 6, 314.
Tourville, J.A., Guenther, F.H., 2011. The DIVA model: a neural theory of speech acquisition and production. Lang. Cogn. Process. 26, 952–981.
Towle, V.L., Bolanos, J., Suarez, D., Tan, K., Grzeszczuk, R., Levin, D.N., Cakmur, R., Frank, S.A., Spire, J.P., 1993. The spatial location of EEG electrodes: locating the best-fitting sphere relative to cortical anatomy. Electroencephalogr. Clin. Neurophysiol. 86, 1–6.
Toyomura, A., Fujii, T., Kuriki, S., 2011. Effect of external auditory pacing on the neural activity of stuttering speakers. NeuroImage 57, 1507–1516.
Vanhoutte, S., Cosyns, M., Van Mierlo, P., Batens, K., Corthals, P., De Letter, M., Van Borsel, J., Santens, P., 2016. When will a stuttering moment occur? The determining role of speech motor preparation. Neuropsychologia 86, 93–102.
Von Holst, E., 1954. Relations between the central nervous system and the peripheral organs. Br. J. Anim. Behav. 2, 89–94.
Wagner, J., Makeig, S., Gola, M., Neuper, C., Muller-Putz, G., 2016. Distinct beta band oscillatory networks subserving motor and cognitive control during gait adaptation. J. Neurosci. 36, 2212–2226.
Walsh, B., Tian, F., Tourville, J.A., Yucel, M.A., Kuczek, T., Bostian, A.J., 2017. Hemodynamics of speech production: an fNIRS investigation of children who stutter. Sci. Rep. 7, 4034.
Watkins, K., 2011. Developmental disorders of speech and language: from genes to brain structure and function. Prog. Brain Res. 189, 225–238.
Watkins, K.E., Smith, S.M., Davis, S., Howell, P., 2008. Structural and functional abnormalities of the motor system in developmental stuttering. Brain 131, 50–59.
Wolpert, D.M., Flanagan, J.R., 2001. Motor prediction. Curr. Biol. 11, R729–R732.
Yairi, E., Ambrose, N., 2013. Epidemiology of stuttering: 21st century advances. J. Fluen. Disord. 38, 66–87.
Yi, W., Qiu, S., Wang, K., Qi, H., He, F., Zhou, P., Zhang, L., Ming, D., 2016. EEG oscillatory patterns and classification of sequential compound limb motor imagery. J. Neuroeng. Rehabil. 13, 11.
Ylinen, S., Nora, A., Leminen, A., Hakala, T., Huotilainen, M., Shtyrov, Y., Makela, J.P., Service, E, 2015. Two distinct auditory-motor circuits for monitoring speech production as revealed by content-specific suppression of auditory cortex. Cereb. Cortex 25, 1576–1586.